Environmental Aspects of Superstatistics: Temperature

G.Cigdem Yalcin[a] , Christian Beck[b]
[a] İstanbul University, Science Faculty, Department of Physics, Vezneciler, İstanbul, Turkey
[b]School of Mathematical Sciences, Queen Mary, University of London, London E1 4NS, UK

"Complex Systems: Foundation and Applications"
The Conference to Celebrate the 70th Birthday of Constantino Tsallis
29th October – 1st November 2013
CBPF - RIO DE JANEIRO - BRAZIL

Superstatistical techniques are powerful tools to describe general classes of complex systems.

The applicability of these techniques to real-world problems is the prominent property of the superstatistics concept.

Some of these numerous interesting applications are;

turbulence
defect turbulence
share price dynamics
random matrix theory
random networks
wind velocity fluctuations
hydro-climatic fluctuations
the statistics of train departure delays
models of the metastatic cascade in cancerous systems
scattering processes in high-energy physics
and complex systems of solid state physics

So far three major physically relevant universality superstatistical classes have been studied:

*χ2 s*uperstatistics, (=Tsallis statistics)

As it is well-known, Superstatistics based on χ2 distributions leads to q-statistics, whereas other distributions lead to something more complicated.

Inverse *χ2* superstatistics,

and

lognormal superstatistics.

These arise as universal limit statistics for many different system (C.Beck, E.G.D. Cohen, H.L.Swinney, PRE 2005):

More recently we have shown that superstatistical techniques could be also successfully applied to environmental aspects of surface temperature distributions.

G.C. Y. and C. Beck, "Environmental Superstatistics", Physica A,392, 5431-5452, 2013

In this work, we have discussed that superstatistical distributions f(β) are very different at different geographic locations, and typically exhibits a double-peak structure for long-term data. For some of our data sets we also find a systematic drift due to global warming.

OUTLINES

- Observed inverse temperature distributions – monthly data
- Observed inverse temperature distributions – yearly data
- Interpretation of results in terms of Köppen-Geiger climate classification system
- Superstatistics with double-peaked distributions
- Global warming

Our superstatistical distributions are consistent with the Köppen-Geiger climate classification system which is one of the most widely used climate classification systems.

There are basically 5 different climatic groups in the Köppen-Geiger scheme:

Group A: Tropical climates
Group B: Arid climates
Group C: Temperate climates
Group D: Cold climates
Group E: Polar climates

We have chosen at least one example in each of these groups:

World map of Köppen-Geiger climate classification

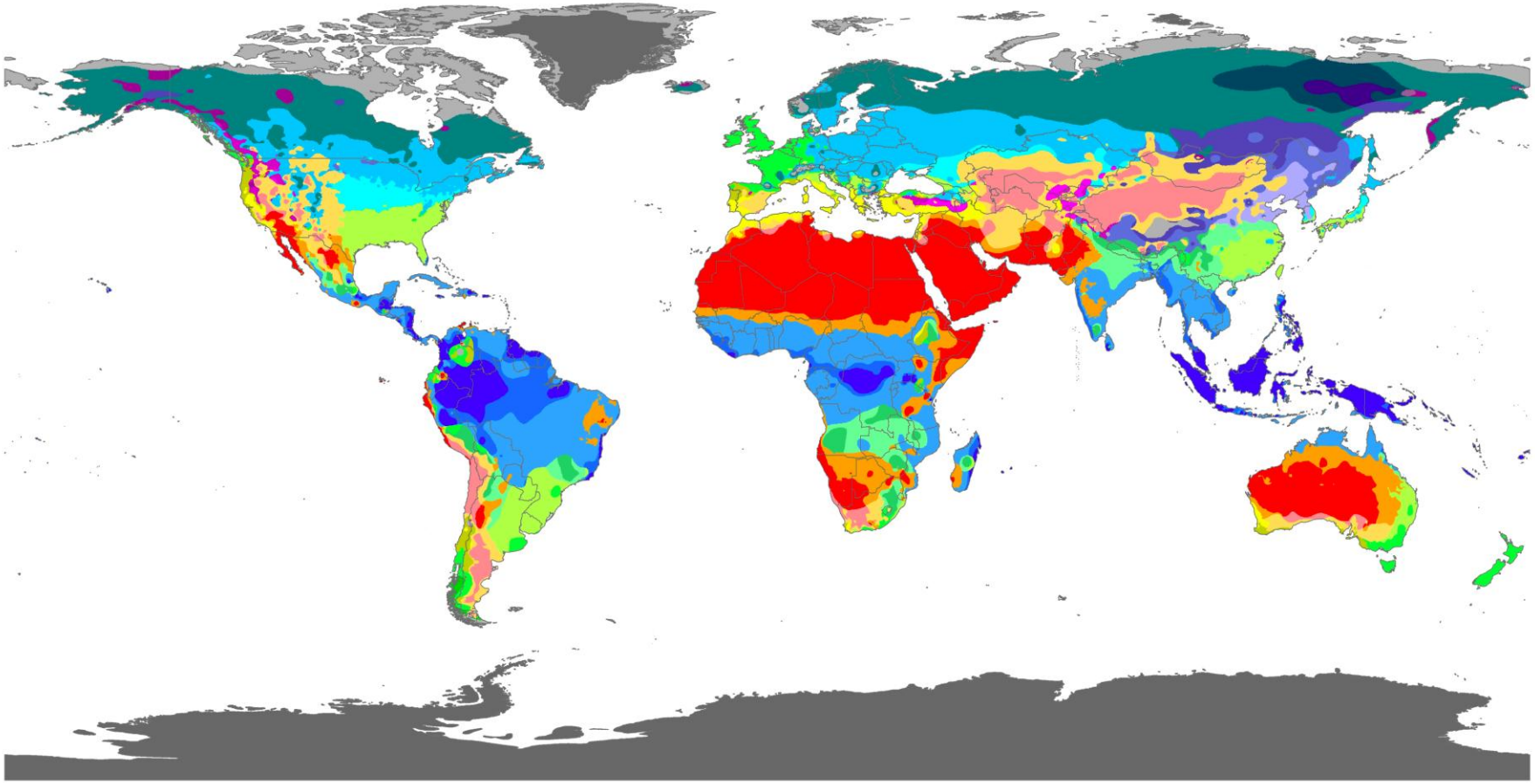

THE UNIVERSITY OF MELBOURNE

Af	BWh	Csa	Cwa	Cfa	Dsa	Dwa	Dfa	ET
Am	BWk	Csb	Cwb	Cfb	Dsb	Dwb	Dfb	EF
Aw	BSh		Cwc	Cfc	Dsc	Dwc	Dfc	
	BSk				Dsd	Dwd	Dfd	

Contact : Murray C. Peel (mpeel@unimelb.edu.au) for further information

DATA SOURCE : GHCN v2.0 station data
Temperature (N = 4,844) and
Precipitation (N = 12,396)

PERIOD OF RECORD : All available

MIN LENGTH : ≥30 for each month.

RESOLUTION : 0.1 degree lat/long

We have investigated time series data for 8 different location in different climatic zones.

Aw (Tropical-Savannah): Darwin (Northern Territory, Australia) (1975-2011)

BSk (Arid-Steppe-Cold): Santa Fe (New Mexico, USA) (1998-2011)

BWh (Arid-Desert-Hot): Dubai (United Arab Emirates) (1974-2011)

Cfa (Temperate-Without dry season-Hot summer): Sydney (New South Wales, Australia) (1910-2011)

Cfb (Temperate-Without dry season-Warm summer):
Central England (London-Bristol-Lancashire) (1910-2011)
Vancouver (British Columbia, Canada) (1937-2011)

Cwa (Temperate-Dry winter-Hot summer): Hong Kong (PRC) (1997-2011)

Dfb (Cold-Without dry season-Warm summer): Ottawa (Ontario, Canada) (1939-2011)

ET(Polar-Tundra): Eureka (Nunavut, Canada) (1951-2011)

We look at monthly data (essentially eliminating seasonal variations) at various geographical locations, and check how well the data are described by Gaussian distributions.

Short-term data temperature distributions (dominated by daily fluctuations) are very different from long-term data (dominated by seasonal variations)

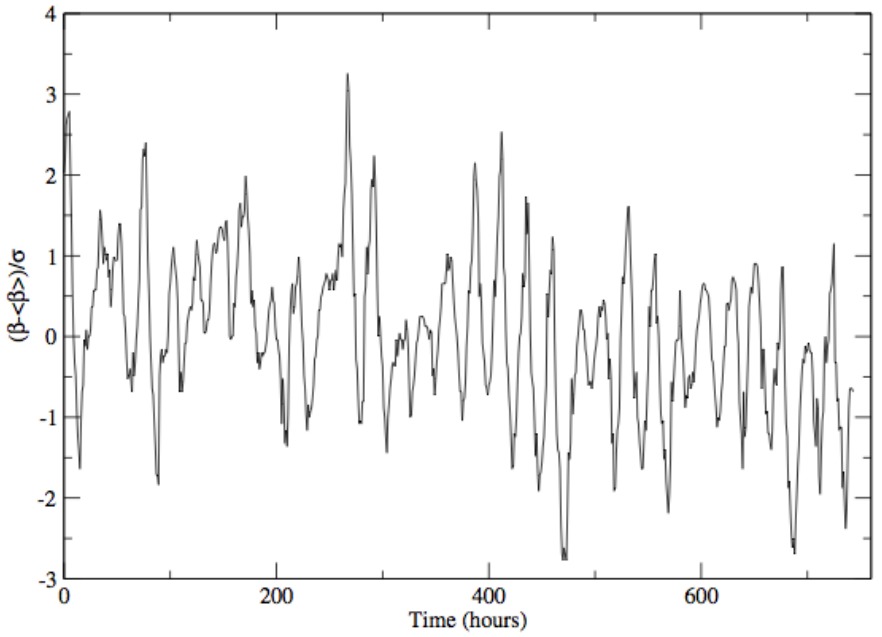

This figure show as an example a time series of hourly measured surface inverse temperature in Vancouver during May 2011.

FIG. 2: Time series of hourly measured inverse temperature in Vancouver during May 2011

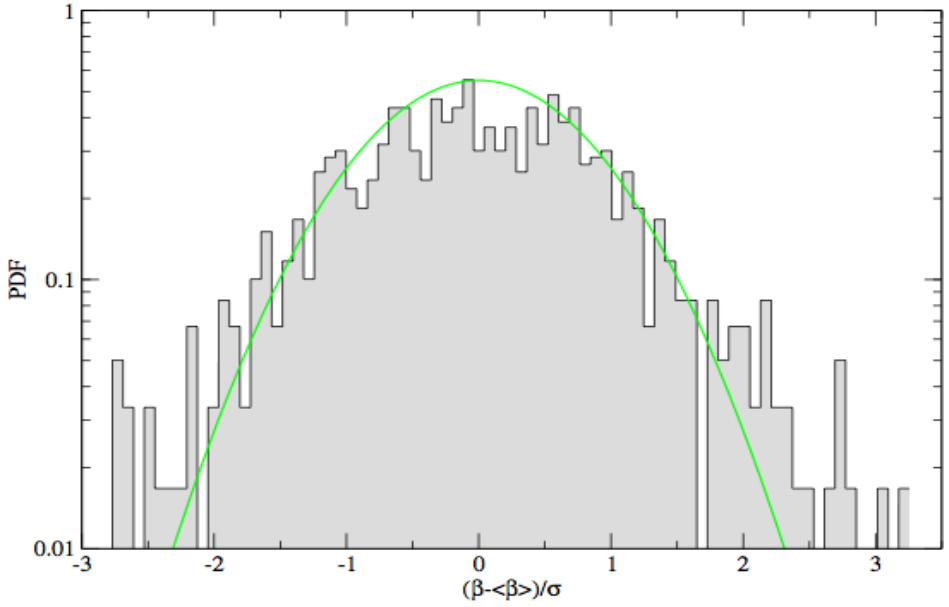

For monthly distributions as displayed in this fig., f(β) is indeed a single-humped probability around the mean inverse temperature that moth, in good approximation given by a Gaussian distribution.

FIG. 5: Gaussian fit to the histogram of the hourly measured inverse temperature in Vancouver during May 2011

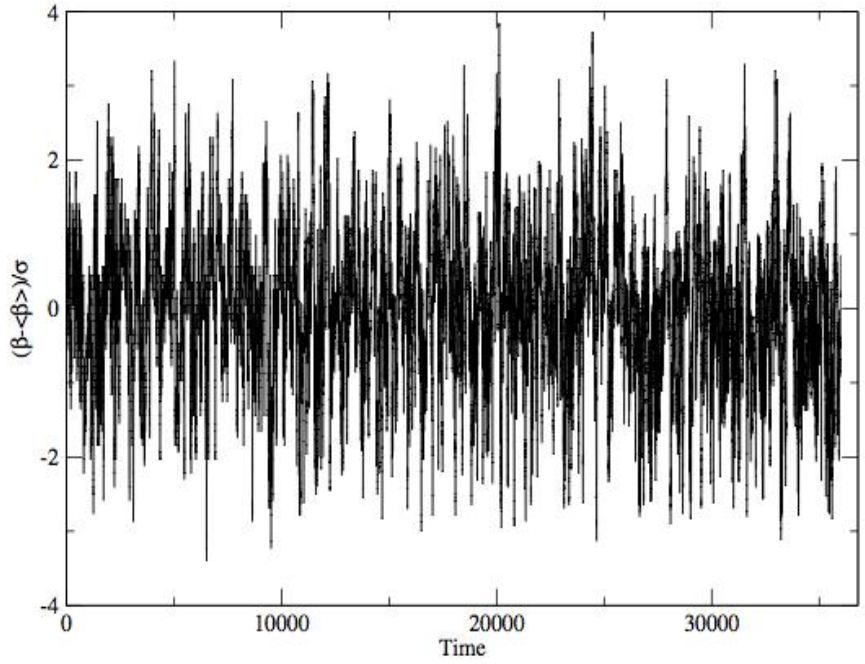

Time series of hourly measured inverse temperature in Ottawa for November, sampled from 1962 to 2011 for 50 years

Better statistics is obtained if we sample the data of a given month over many years.

We sampled hourly measured inverse temperature time series, restricted to the month of November, over the period 1966-2011 for Ottawa.

This figure shows this time series (restricted to November months and joined together).

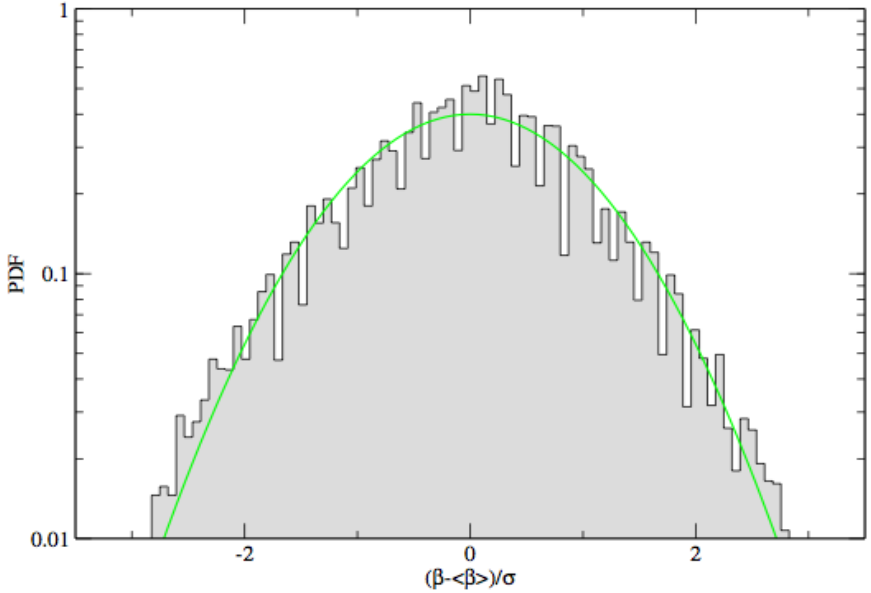

: Gaussian fit to the histogram of the hourly measured inverse temperature in Ottawa for 50 November months

The corresponding histogram is well-fitted by a Gaussian.

We analyse in detail inverse temperature distributions at various geographic locations. These environmentally important distributions are different from standard examples of distribution functions discussed so far in the literature, such as the $\chi 2$, inverse $\chi 2$ or lognormal distribution.

A major difference is that the environmentally observed probability densities of inverse temperature typically exhibit a double-peak structure, thus requiring a different type of superstatistics than what has been done so far.

We look at long-term data including seasonal variations, which induce double-peaked distributions, but with specific differences at different geographical locations, depending on local climate.

Apparently environmental superstatistics does not have sharply peaked distributions f(β), but we will see there are broad distributions that often have two maxima. Hence the effective Boltzmann factors

$$B(E) = \int_0^\infty \mathrm{d}\beta f(\beta)\, \mathrm{e}^{-\beta E}$$

can only be evaluated numerically.

One idea would be effectively separate the two maxima and to do a superposition of two single peaked superstatistics, one for the summer and one for the winter.


Basilan
Malaysia
Kuala Lumpur
Singapore
Java Sea
Jakarta
Surabaya
Indonesia
Banda Sea
Bismarck Sea
Papua New Guinea
Arafura Sea
A
Timor Sea
Northern Territory
Queensland
Australia
Western Australia
Brisbane
South Australia
Perth
New South Wales
Sydney
Great Australian Bight
Australian Capital Territory
Victoria
Melbourne

For tropical locations, such as Darwin , the two peaks merge in a single peak, as expected for regions where there is hardly any difference between summer and winter temperatures.

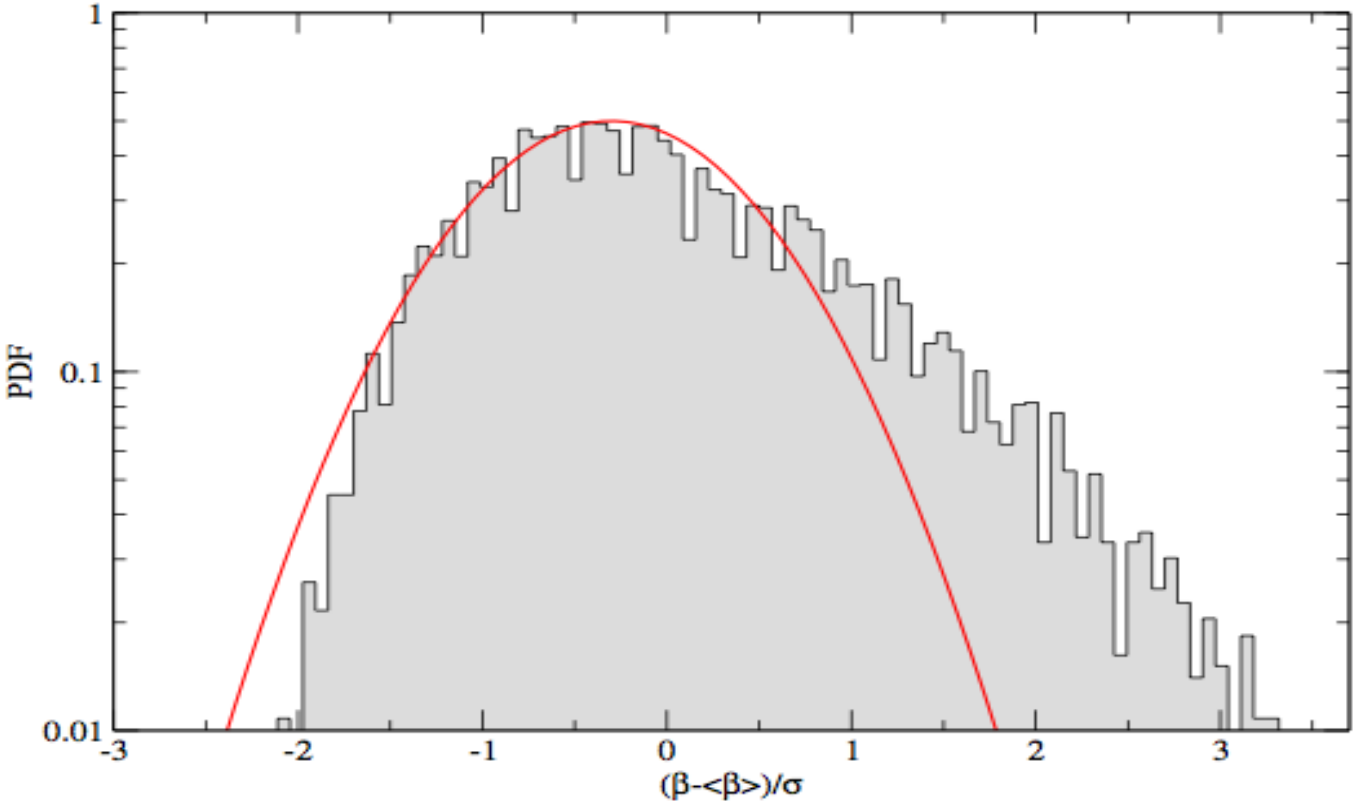

FIG. 22: Distribution of the daily measured inverse mean temperature in Darwin for 1975-2011

Calgary
Winnipeg
Vancouver
Washington
Montana
North Dakota
Minnesota
South Dakota
Wisconsin
Oregon
Idaho
Wyoming
Nebraska
Iowa
Illinois
Ohio
Indiana
New York
Massachusetts
Rhode Island
Connecticut
New Jersey
Delaware
Maryland
District of Columbia
West Virginia
Virginia
Kentucky
North Carolina
South Carolina
Tennessee
Nevada
Utah
Colorado
Kansas
Missouri
Oklahoma
Arkansas
Mississippi
Alabama
Georgia
Florida
Louisiana
Texas
United States
San Francisco
California
Los Angeles
San Diego
Arizona
Phoenix
New Mexico
Dallas
San Antonio
Houston
Monterrey
Gulf of California
Gulf of Mexico
México
Havana
A

A typical observation is now that the relevant distributions have a double-peak structure, at least for non-tropical locations.

Broadly, the left peak corresponds to summer and the right peak to winter.

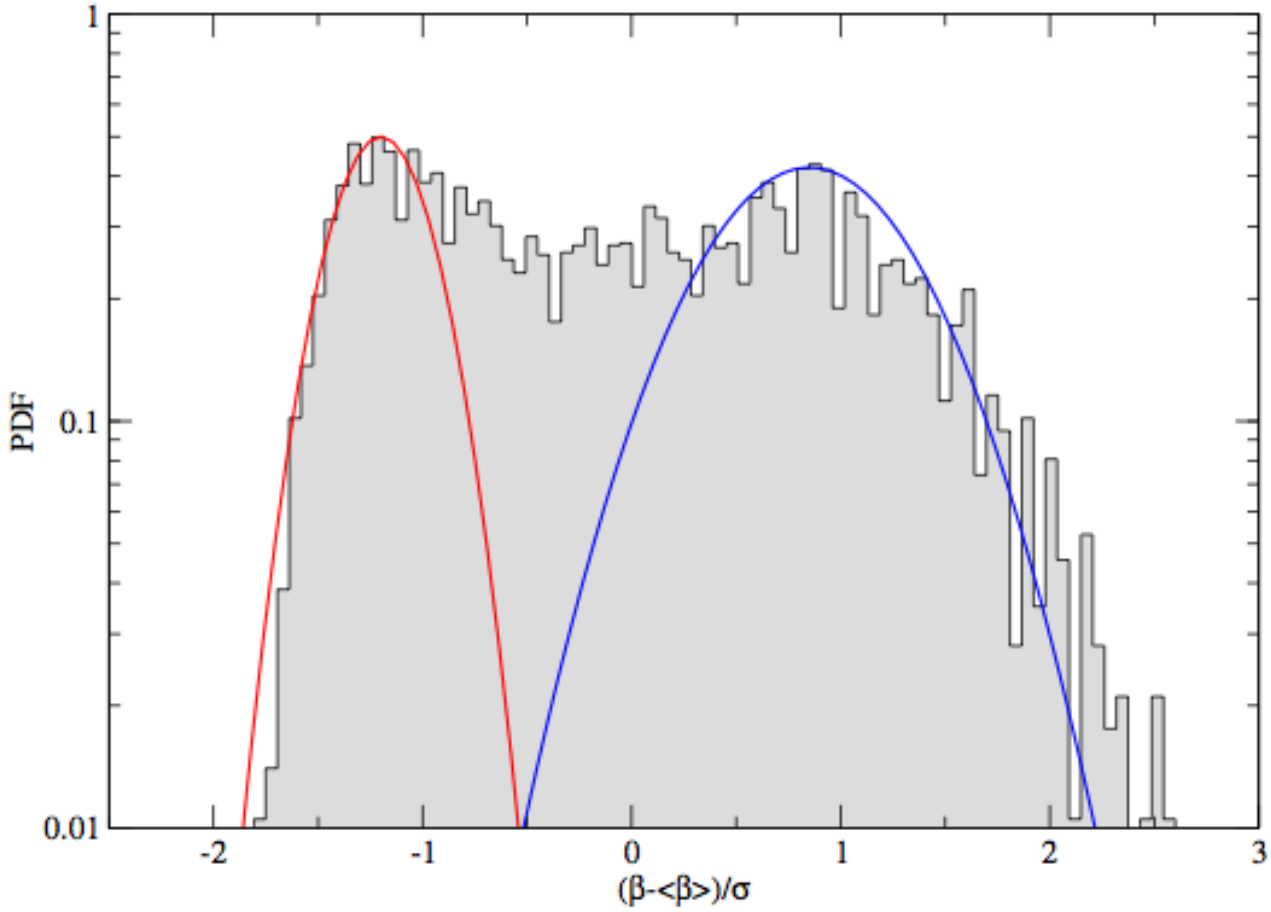

FIG. 23: Distribution of the daily measured inverse mean temperature in Santa Fe for 1998-2011

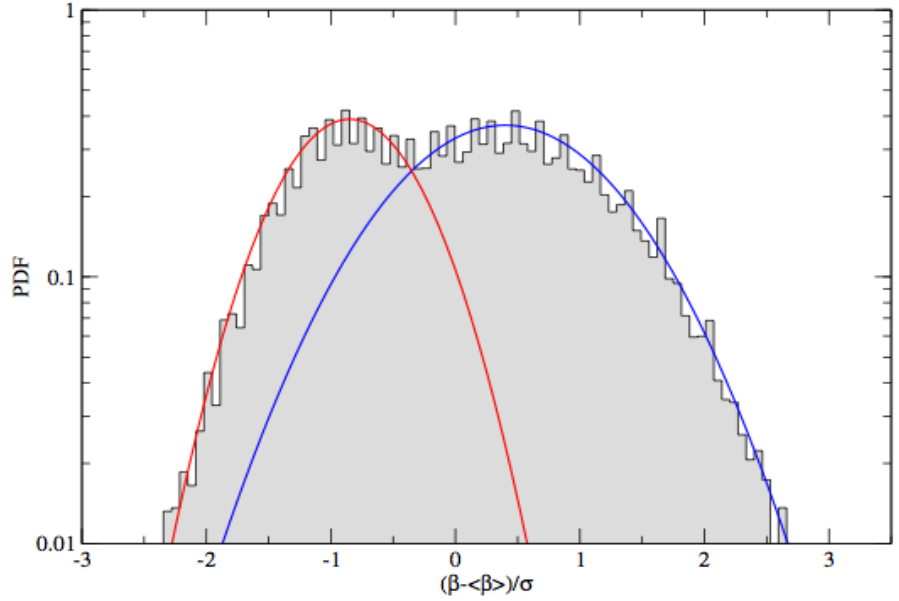

FIG. 26: Distribution of the daily measured inverse mean temperature in Central England (Lancashire, London and Bristol) for 1910-2011

The plots of Central England and Vancouver are very similar.

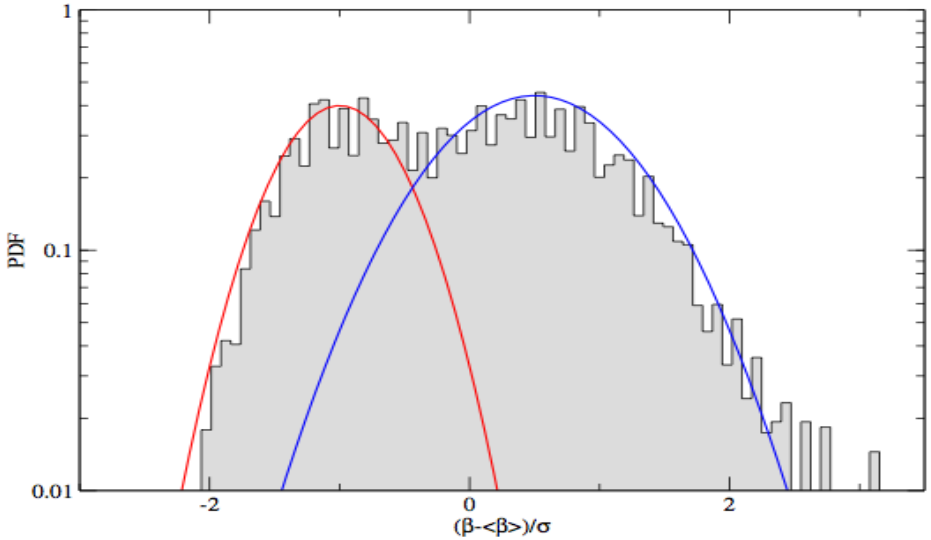

FIG. 27: Distribution of the daily measured inverse mean temperature in Vancouver for 1937-2011

This is to be expected, since both locations fall into the same climate type Cfb

For example, Sydney seems special since it is the only example where the summer-Gaussian has significantly higher variance than the winter-Gaussian.

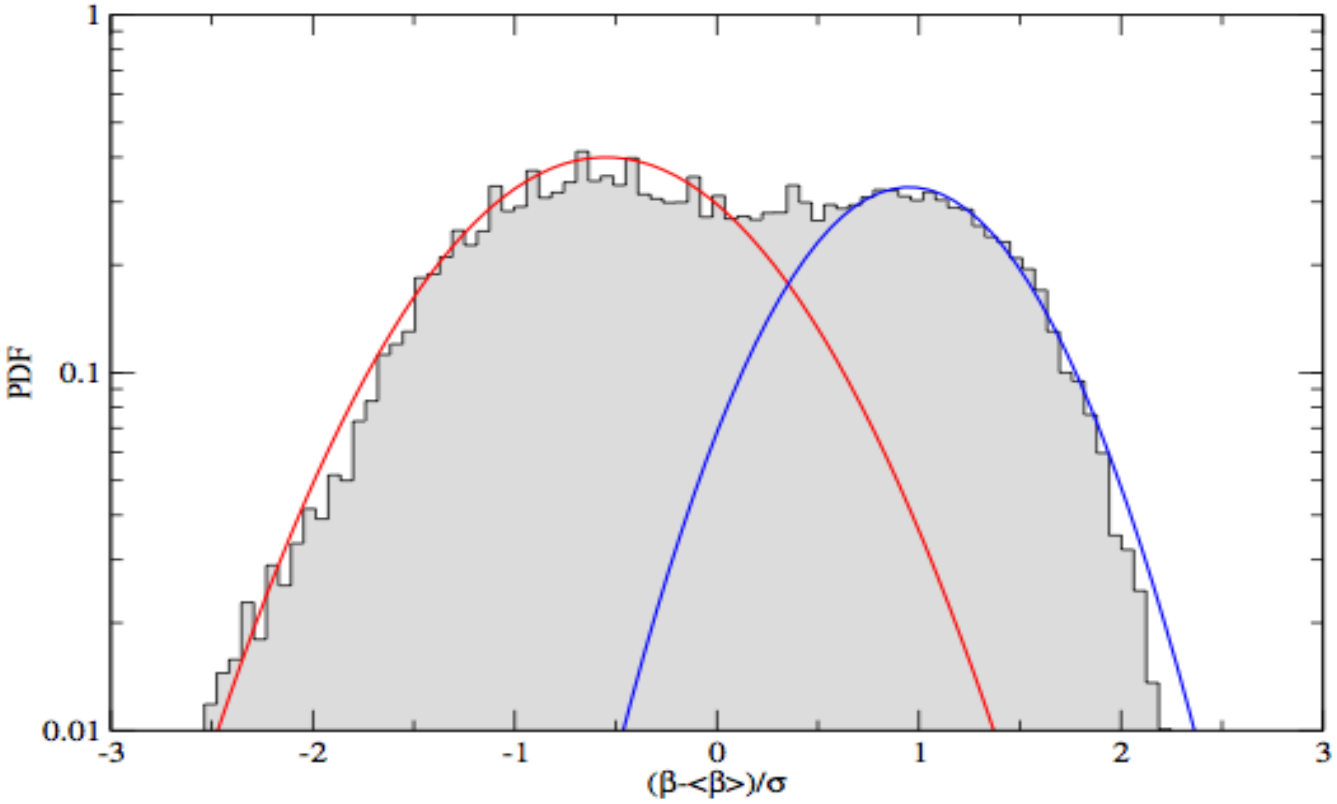

FIG. 25: Distribution of the daily measured inverse mean temperature in Sydney for 1910-2011

The entire distribution can be very roughly regarded as a superposition of two Gaussians, with intermediate behaviour between the peaks.

Dubai seems special as well, since both winter and summer-Gaussian seem to have roughly the same variance. This allows for an alternative fit with the exponential of a double-well potential.

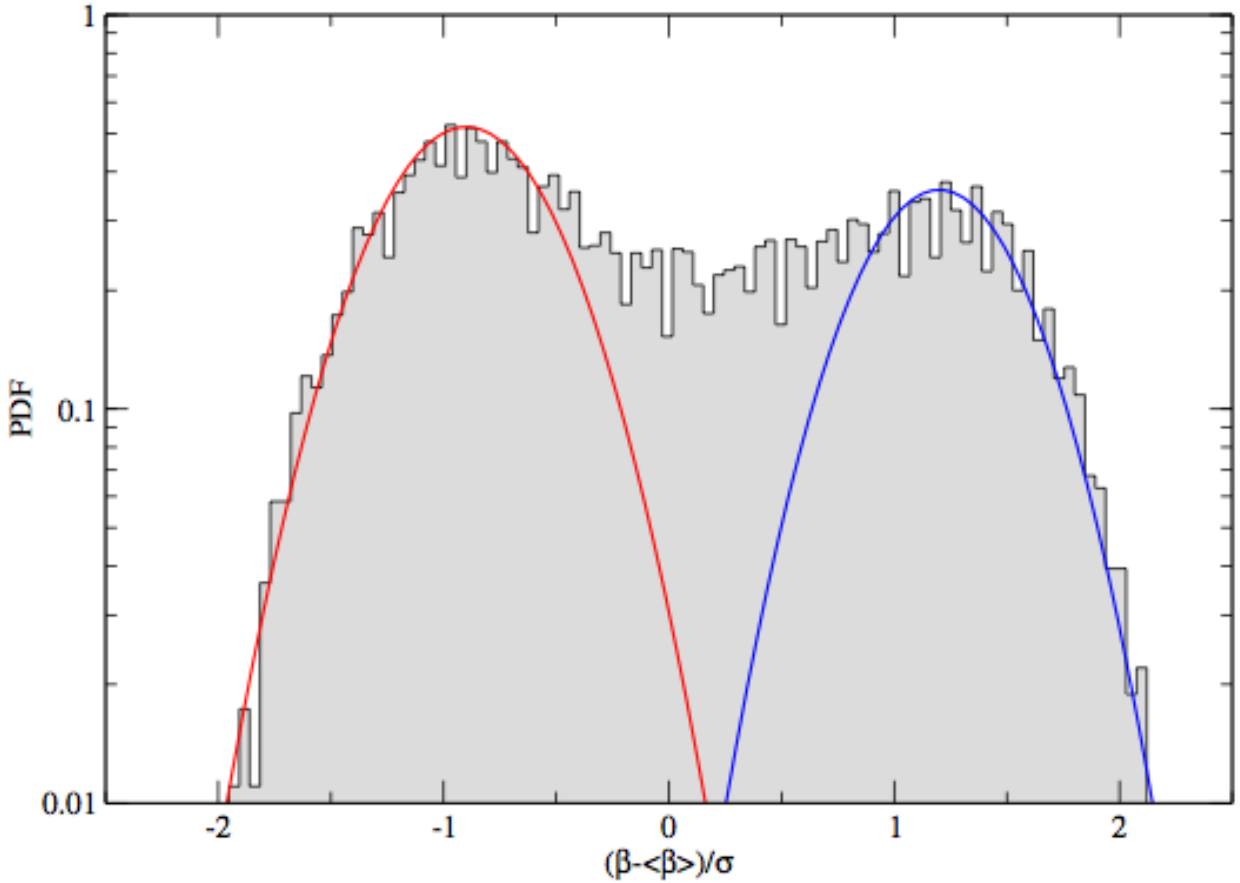

FIG. 24: Distribution of the daily measured inverse mean temperature in Dubai for 1974-2011

One may try to fit the data by other functional forms than a superposition of two Gaussians. For example, the histogram of daily measured inverse temperature in Dubai (1974-2011) is well fitted by an exponential $e^{-V(\beta)}$ of a double-well potential $V(x) \sim (C_2x^2+C_3x^{3+}C_4x^4)$.

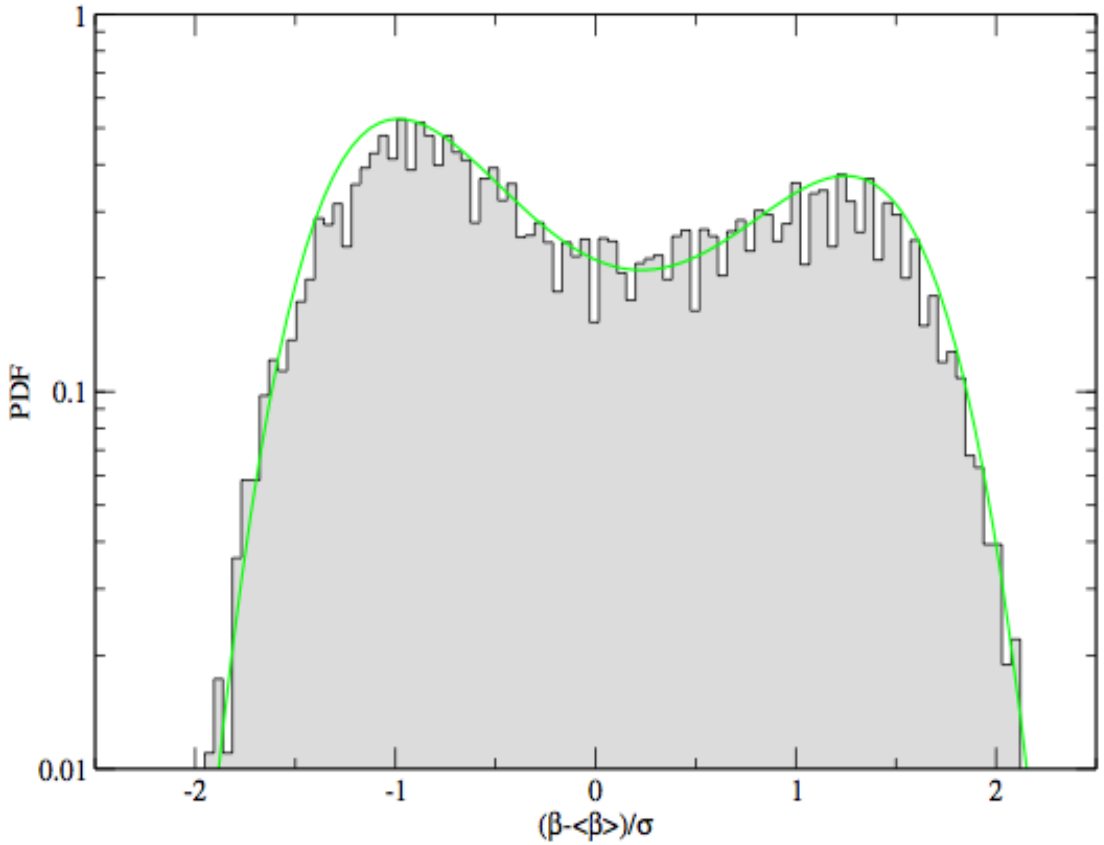

FIG. 31: Fit with the exponential of a double-well potential to the histogram of the daily measured inverse mean temperature in Dubai 1974-2011


A
Arctic Ocean
Baffin Bay
Kalaallit Nunaat
(Greenland)
Ísland
(Iceland)
Northwestern Passages
NU
NT
YT
AK
Canada
Hudson Bay
Gulf of Alaska
AB
MB
BC
SK
NL

For polar locations, the two peaks are strongly separated, as shown in the Fig. for the example of Eureka. Here the two Gaussians are very far apart from each other.

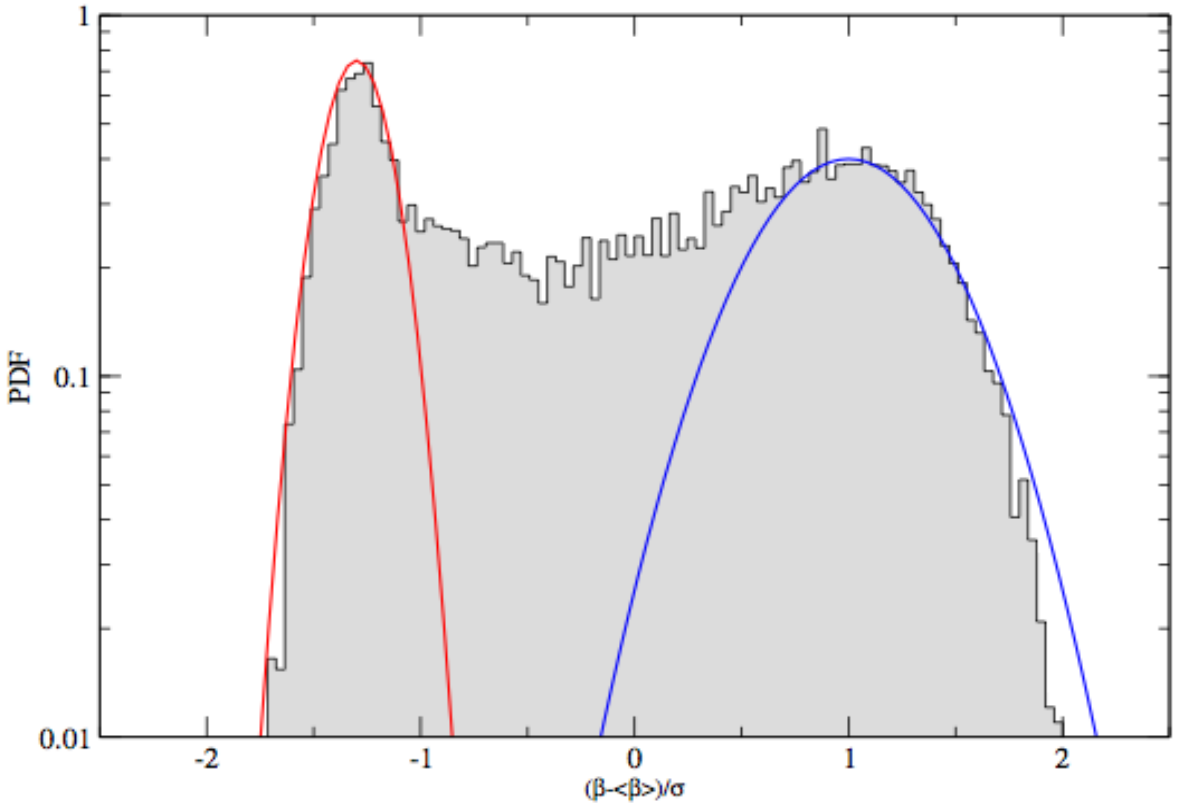

FIG. 30: Distribution of the daily measured inverse mean temperature in Eureka for 1951-2011

The intermediate behaviour between the peak is more pronounced for geographical locations that have a big differences between summer and winter temperatures.

Location and time period	*Summer(Celcius)*	*Winter(Celcius)*	β_1	β_2
Darwin (1975-2011)	28.32	-	1.8	-
Santa Fe (1998-2011)	22.06	3.31	18	4
Dubai (1974-2011)	33.03	20.39	7	8
Sydney (1910-2011)	20.22	13.78	2	3.5
Central England (1910-2011)	14.26	7.12	3.6	1.4
Vancouver (1937-2011)	15.80	7.05	5	2
Hong Kong (1997-2011)	27.99	19.31	10	2.7
Ottawa (1939-2011)	18.49	-1.04	12	2.1
Eureka (1951-2011)	4.21	-36.3	43	5.5

TABLE I: Maxima (in degree Celsius) and variance parameters β_1, β_2 of the two Gaussians $\sim e^{-\beta_i(\beta-\bar{\beta})^2}$ used in the fits.

The table lists the two temperatures where the two maxima in histogram occur.

They are consistent with an average temperature observed during a couple of months corresponding to summer and winter, respectively, at different geographical locations.

In some of our data one sees a systematic trend which can be associated with global warming. As it is well-known, global warming is the rise in the average temperature of the Earth's atmosphere and of the oceans since the late 19th century and its projected continuation.

Quantitatively, the Earth's average surface temperature rose by 0.74±0.18 ◦C over the period 1906-2005. The rate of warming over the last half of that period was almost double that of the period as a whole (0.13±0.03◦C per decade, versus 0.07±0.02 ◦C per decade).

Arctic regions are especially vulnerable to the effects of global warming, as has become apparent in the melting sea ice in recent years. Climate models predict much greater warming in the Arctic than the global average.

If sampled over many decades, the precision of some of our data is good enough to reveal the effects of global warming. As an example we show that the average of daily measured mean temperature of every single year in Eureka, Nunavut, Canada from 1951-2011. This is an arctic region and our plot shows that the average temperature grows by 0.92 ◦C per decade. So in this polar region the warming occurs at a much higher rate than global warming rate that is averaged over the entire earth.

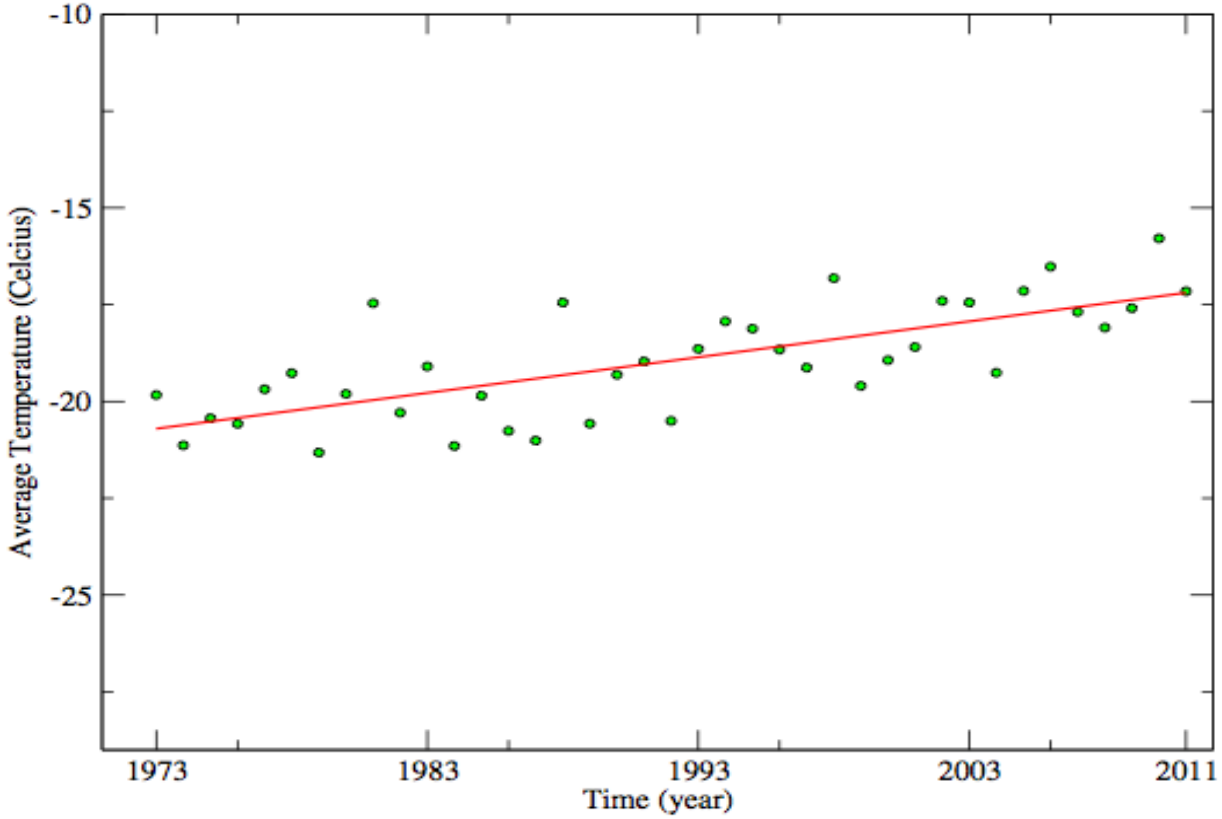

FIG. 33: Average of daily measured mean temperature of every single year in Eureka 1973-2011

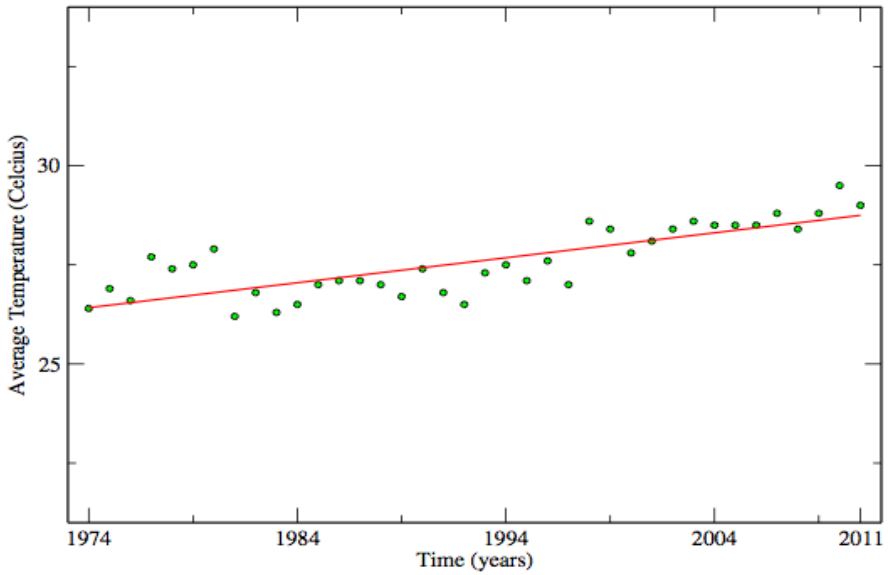

FIG. 34: Average of daily measured mean temperature of every single year in Dubai 1974-2011

For some of the other locations we also observe a systematic increase in average temperature . For Dubai the rate is also rather high, 0.63 ◦C per decade.

For Sydney , the average global warming rate 0.13 ◦C per decade.

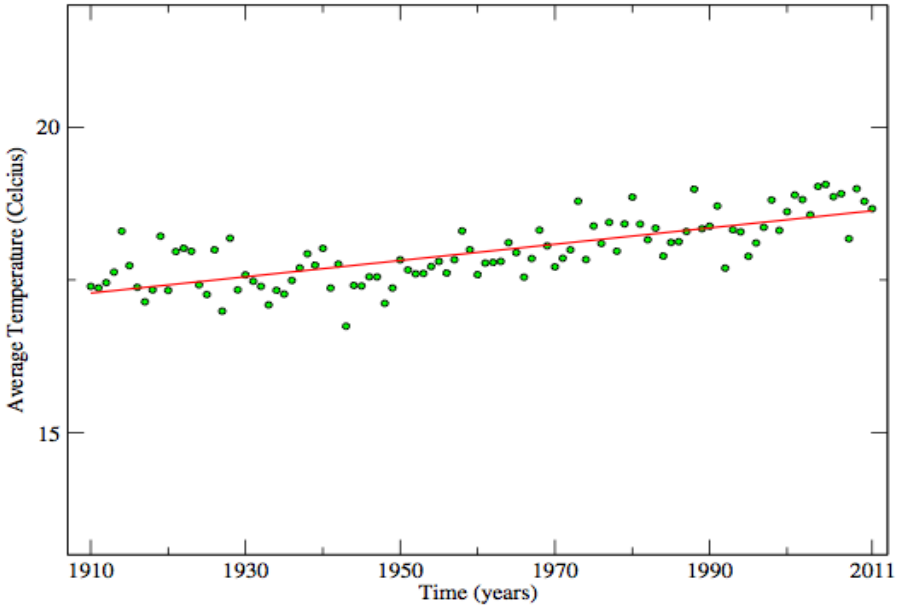

FIG. 35: Average of daily measured mean temperature of every single year in Sydney 1910-2011

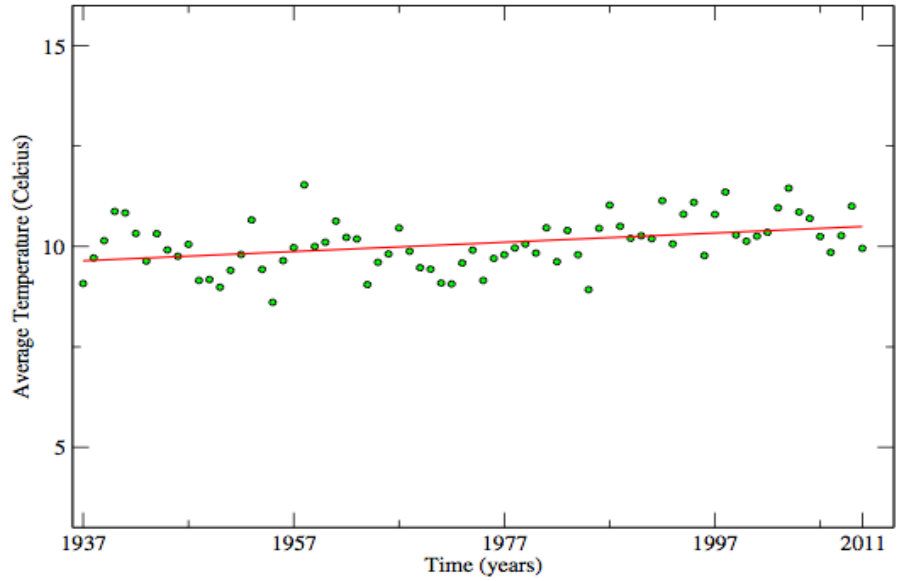

FIG. 36: Average of daily measured mean temperature of every single year in Vancouver 1937-2011

For Vancouver, the average global warming rate 0.11 ◦C per decade.

For Ottawa the average global warming rate 0.18 ◦C per decade.

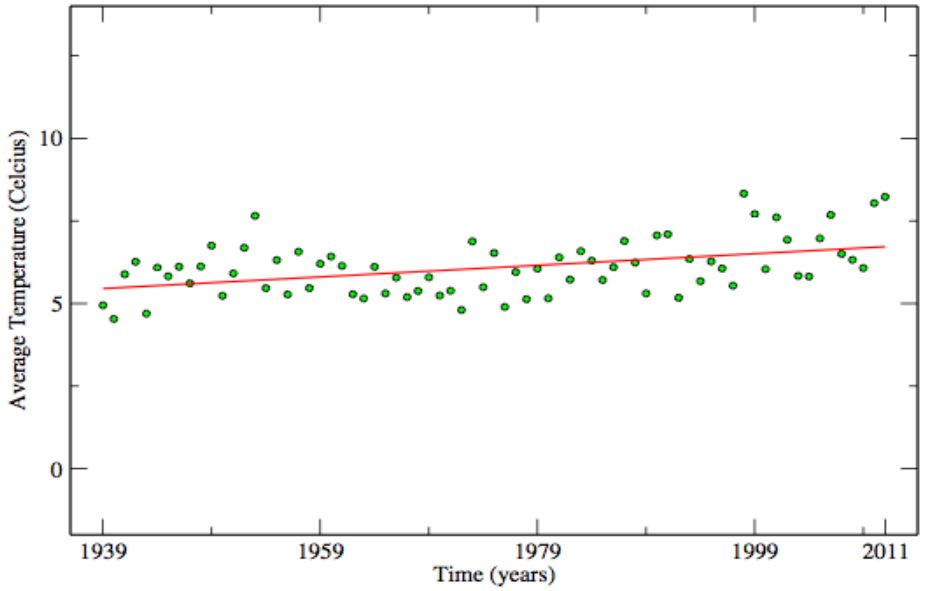

FIG. 37: Average of daily measured mean temperature of every single year in Ottawa 1939-2011

CONCLUSIONS

◆ Our superstatistical distributions are consistent with the Köppen-Geiger climate classification system which is one of the most widely used climate classification systems.

◆ The details of the distribution of course heavily depend on the climate zone of the location.

◆ These environmentally important distributions are different from standard examples of distribution functions discussed so far in the literature, such as the $\chi 2$, inverse $\chi 2$ or lognormal distribution.

◆ So far our investigation only involves temperature distributions.
In future work, we intend to take into account some other environmental parameters as well, which can also be modelled using superstatistical techniques.

Thank you

:-)

Happy Birthday to Prof.Constantino Tsallis